THE JOURNAL OF BIOLOGICAL CHEMISTRY VOL. 282, NO. 38, pp. 27875–27886, September 21, 2007

Gangliosides and Nogo Receptors Independently Mediate Myelin-associated Glycoprotein Inhibition of Neurite Outgrowth in Different Nerve Cells*

Received for publication, May 16, 2007, and in revised form, July 5, 2007 Published, JBC Papers in Press, July 19, 2007, DOI 10.1074/jbc.M704055200

Niraj R. Mehta[‡1], **Pablo H. H. Lopez**[‡], **Alka A. Vyas**[‡2], **and Ronald L. Schnaar**[‡§3]

From the Departments of [‡]*Pharmacology and* [§]*Neuroscience, The Johns Hopkins School of Medicine, Baltimore, Maryland 21205*

In the injured nervous system, myelin-associated glycoprotein (MAG) on residual myelin binds to receptors on axons, inhibits axon outgrowth, and limits functional recovery. Conflicting reports identify gangliosides (GD1a and GT1b) and glycosylphosphatidylinositol-anchored Nogo receptors (NgRs) as exclusive axonal receptors for MAG. We used enzymes and pharmacological agents to distinguish the relative roles of gangliosides and NgRs in MAG-mediated inhibition of neurite outgrowth from three nerve cell types, dorsal root ganglion neurons (DRGNs), cerebellar granule neurons (CGNs), and hippocampal neurons. Primary rat neurons were cultured on control substrata and substrata adsorbed with full-length native MAG extracted from purified myelin. The receptors responsible for MAG inhibition of neurite outgrowth varied with nerve cell type. In DRGNs, most of the MAG inhibition was via NgRs, evidenced by reversal of inhibition by phosphatidylinositol-specific phospholipase C (PI-PLC), which cleaves glycosylphosphatidylinositol anchors, or by NEP1–40, a peptide inhibitor of NgR. A smaller percentage of MAG inhibition of DRGN outgrowth was via gangliosides, evidenced by partial reversal by addition of sialidase to cleave GD1a and GT1b or by P4, an inhibitor of ganglioside biosynthesis. Combining either PI-PLC and sialidase or NEP1–40 and P4 was additive. In contrast to DRGNs, in CGNs MAG inhibition was exclusively via gangliosides, whereas inhibition of hippocampal neuron outgrowth was mostly reversed by sialidase or P4 and only modestly reversed by PI-PLC or NEP1–40 in a non-additive fashion. A soluble proteolytic fragment of native MAG, dMAG, also inhibited neurite outgrowth. In DRGNs, dMAG inhibition was exclusively NgR-dependent, whereas in CGNs it was exclusively ganglioside-dependent. An inhibitor of Rho kinase reversed MAG-mediated inhibition in all nerve cells, whereas a peptide inhibitor of the transducer $p75^{NTR}$ had cell-specific effects quantitatively similar to NgR blockers. Our data indicate that MAG inhibits axon outgrowth via two independent receptors, gangliosides and NgRs.

The injured adult mammalian central nervous system is a highly inhibitory environment for axon regeneration due in part to endogenous axon regeneration inhibitors (ARIs)[4] at least three of which are expressed on residual myelin that persists at sites of central nervous system injury (1, 2). Knowledge of myelin-derived ARIs, their receptors on axons, and the downstream signaling pathways that limit axon outgrowth may provide new opportunities to reverse inhibition and enhance recovery after traumatic central nervous system injury (3, 4). One well established inhibitor of axon regeneration is myelin-associated glycoprotein (MAG), a transmembrane protein of the immunoglobulin superfamily that is expressed on the innermost wrap of myelin directly apposed to the axon surface. MAG is essential to the long term stability of myelinated axons and positively regulates axon cytoarchitecture (5). However, in the injured nervous system, MAG on residual myelin membranes at sites of injury, as well as a proteolytic fragment of MAG released into the surrounding milieu, binds to receptors on axons resulting in activation of RhoA and halting axon outgrowth (6–9).

The identity of the axonal receptors for MAG has been a matter of controversy. As a member of the Siglec family of sialic acid-binding lectins, MAG binds with selectivity to two closely related major sialoglycans expressed on axons and neurons throughout the brain, gangliosides GD1a and GT1b (10, 11). Functional studies using cultured neurons revealed that gangliosides are required for MAG-mediated inhibition of axon outgrowth and that interfering with ganglioside expression or blocking MAG-ganglioside binding reversed inhibition (12). Subsequent studies, however, identified a glycosylphosphatidylinositol (GPI)-anchored protein, Nogo receptor (NgR)[5], as the essential high affinity MAG receptor (13, 14). These studies reported that sialoglycans, including gangliosides, were not involved in MAG inhibition of axon outgrowth (although conflicting data on the role of sialoglycans in NgR binding have

* This work was supported in part by National Institutes of Health Grant R37NS037096. The costs of publication of this article were defrayed in part by the payment of page charges. This article must therefore be hereby marked "*advertisement*" in accordance with 18 U.S.C. Section 1734 solely to indicate this fact.

[1] A fellow of the National Institutes of Health-supported Pharmacology Training Program (Grant T32GM008763).

[2] Supported in part by a Whittaker Foundation fellowship.

[3] To whom correspondence should be addressed: Dept. of Pharmacology and Molecular Sciences, The Johns Hopkins School of Medicine, 725 N. Wolfe St., Baltimore, MD 21205. Tel.: 410-955-8392; Fax: 410-955-4900; E-mail: schnaar@jhu.edu.

[4] The abbreviations used are: ARI, axon regeneration inhibitor; CGN, cerebellar granule neuron; CHO, Chinese hamster ovary; dMAG, soluble proteolytic fragment of myelin-associated glycoprotein; DRGN, dorsal root ganglion neuron; GPI, glycosylphosphatidylinositol; HN, hippocampal neuron; mAb, monoclonal antibody; MAG, myelin-associated glycoprotein; NEP1–40, Nogo extracellular peptide, residues 1–40; NgR, Nogo receptor; P4, (1*R*,2*R*)-1-phenyl-2-hexadecanoylamino-3-pyrrolidino-1-propanol; PI-PLC, phosphatidylinositol-specific phospholipase C. Ganglioside nomenclature is that of Svennerholm (54).

[5] The NgR family consists of three related proteins, NgR (NgR1), NgR2, and NgR3. When used, the term "NgRs" in this paper refers to the two members, NgR1 and NgR2, that bind MAG and have been shown to mediate MAG inhibition of neurite outgrowth (13–15, 46).

appeared (15)). In an effort to reconcile these discrepancies, we considered whether gangliosides and NgRs function independently or cooperatively on different nerve cell types or in response to different physical forms of MAG (membrane-bound and soluble). Our results indicate that gangliosides and NgRs can act independently as receptors for both membrane-bound and soluble forms of MAG and that different nerve cell types use different MAG receptors.

EXPERIMENTAL PROCEDURES

Materials—Phosphatidylinositol-specific phospholipase C (PI-PLC; *Bacillus cereus*) and Y-27632 (Rho kinase inhibitor) were from Sigma-Aldrich. NEP1–40 (NgR-blocking peptide) and TAT-Pep5 (cell-permeable $p75^{NTR}$ signaling inhibitor (16)) were from EMD Biosciences, La Jolla, CA. A scrambled control peptide for NEP1–40 (17) was from Alpha Diagnostic International, San Antonio, TX. Sialidase (*Vibrio cholerae*) was overexpressed in *Escherichia coli* using an expression plasmid (pET30 b(+)/VCNA) kindly provided by Dr. G. Taylor, University of St. Andrews, Fife, Scotland, UK, and was purified as described previously (18). Anti-MAG monoclonal antibody (mAb) 513 was generated from the hybridoma, a kind gift of Dr. M. Schachner, Hamburg University, as described previously (19). The glycosphingolipid biosynthesis inhibitor (1*R*,2*R*)-1-phenyl-2-hexadecanoylamino-3-pyrrolidino-1-propanol (P4) was synthesized by Dr. D. Meyers, Synthetic Core Facility, The Johns Hopkins School of Medicine, Baltimore, MD.

Dorsal Root Ganglion Neurons (DRGNs)—Cells were prepared using a protocol adapted from Li *et al.* (20). Dorsal root ganglia, dissected from 5–6-day-old Sprague-Dawley rats, were treated at 37 °C with 2 mg/ml collagenase (Worthington) in L-15 medium (Invitrogen) for 30 min. The collagenase solution was decanted and replaced with a solution of 2.5 mg/ml trypsin and 1 mM EDTA (Invitrogen). After 45 min at 37 °C, soybean trypsin inhibitor (2.5 mg/ml, Sigma-Aldrich) was added, and the tissue was mechanically disaggregated by trituration with a fire-polished Pasteur pipette. Cells were collected by centrifugation (500 × *g* for 7 min) and resuspended in growth medium (Neurobasal medium (Invitrogen) containing 0.13 mM L-glutamine, 0.25% (v/v) heat-inactivated fetal bovine serum (Hyclone, Logan, UT), 0.5% B-27 supplement (Invitrogen), 100 units/ml penicillin, and 100 μg/ml streptomycin). Cell aggregates were removed by passing through a 40-μm cell strainer (BD Biosciences), and the dissociated cells were plated on a 35-mm cell culture dish coated with 10 μg/ml laminin (Trevigen, Gaithersburg, MD) for 1 h at 37 °C. Non-adherent cells were collected and diluted in growth medium further supplemented with 50 ng/ml murine nerve growth factor (BD Biosciences). Cells were plated (10,000 cells in 100 μl/well) on a 96-well plate (Costar, Corning, NY) pretreated for 1 h with 45 μg/ml poly-D-lysine (Sigma) (molecular weight, 30,000–70,000) and cultured at 37 °C in a 5% CO_2 incubator for 18–24 h.

Cerebellar Granule Neurons (CGNs)—Cell isolation was as described previously (21, 22). Cerebella were collected from postnatal day 4–5 rats, meninges were removed, and the tissue was dissociated using a Papain Dissociation kit (Worthington). Briefly tissue was treated with 20 units/ml papain and 0.05 mg/ml DNase at 37 °C for 30 min and triturated with a fire-polished Pasteur pipette. Cells were collected by centrifugation (300 × *g* for 7 min), and the pellet was resuspended in buffer containing ovomucoid. Cells were collected by centrifugation, resuspended in growth medium (minimal essential medium (Invitrogen) containing 25 mM Hepes, 25 mM KCl, 10% (v/v) heat-inactivated horse serum, 5% (v/v) fetal bovine serum (Hyclone), 100 units/ml penicillin, 100 μg/ml streptomycin, and 2 mM L-glutamine), plated (55,000 cells in 100 μl/well) on 96-well plates (Nunc, Roskilde, Denmark) precoated with 125 μg/ml poly-D-lysine (molecular weight, >300,000), and cultured at 37 °C in a 5% CO_2 incubator for 48 h.

Hippocampal Neurons (HNs)—Rat hippocampal neurons were prepared essentially as described previously (23). Hippocampi of postnatal day 4–5 rats were dissected into ice-cold medium (98% HibernateA (BrainBits, Springfield, IL) and 2% B-27 supplement). After removal of meninges, the tissue was cut into small pieces, and then papain (Worthington, 2 mg/ml in medium) was added. After 30 min at 37 °C with gentle agitation, the tissue was allowed to settle, the papain solution was decanted, and medium was added. After 5 min at ambient temperature, tissue was disaggregated using a fire-polished Pasteur pipette, and the cell suspension was layered above a solution of 15% Nycodenz (Axis-Shield, Oslo, Norway) in medium and centrifuged (800 × *g* for 15 min) at ambient temperature. Cells were resuspended in HibernateA, collected by centrifugation, and resuspended in growth medium (NeurobasalA (Invitrogen):B-27 (400:1) supplemented with 0.5 mM glutamine, 100 units/ml penicillin, 100 μg/ml streptomycin, and 5 ng/ml fibroblast growth factor 2 (Chemicon, Temecula, CA)). Cells were passed through a 40-μm cell strainer, plated (20,000 cells in 100 μl/well) on 96-well plates (Nunc) previously coated for 1 h with 125 μg/ml poly-D-lysine (molecular weight, >300,000), and cultured at 37 °C in a 5% CO_2 incubator for 48 h.

Inhibitory Substrata—MAG was extracted from purified myelin membranes using mild detergent and adsorbed to culture surfaces as described previously (12). Briefly myelin was purified (24) from brains freshly dissected from adult Sprague-Dawley rats or adult wild type or MAG-null mice (25) and stored at −70 °C prior to use. Myelin membranes were suspended at 1 mg of protein/ml in extraction buffer (0.2 M sodium phosphate buffer (pH 6.8), 0.1 M Na_2SO_4, 1 mM EDTA, 1 mM dithiothreitol, protease inhibitor mixture (Sigma), and 1% octylglucoside), incubated at 4 °C for 16 h with gentle agitation, and then centrifuged at 100,000 × *g* for 1 h at 4 °C. The supernatant was collected and diluted with an equal volume of detergent-free buffer, and an aliquot (50 μl) was added to each well of a poly-D-lysine-coated 96-well plate (see above). After 4 h at ambient temperature, the plate was washed with Dulbecco's phosphate-buffered saline and then with the culture medium appropriate to the cell type (see above) prior to plating freshly prepared cells.

Soluble Proteolytic Fragment of Myelin-associated Glycoprotein (dMAG)—Spontaneously generated dMAG was prepared essentially as described previously (8). Rat brain myelin was purified as described above except that protease inhibitors were

omitted. Freshly purified myelin membrane was resuspended in Neurobasal medium. Aliquots containing 4–5 mg of myelin protein in 0.3 ml of Neurobasal medium were incubated at ambient temperature or 37 °C for 18–24 h. Membranes were removed by centrifugation (100,000 × *g* for 1 h at 4 °C). The supernatant, containing spontaneously released proteolytic MAG fragment, was diluted 8-fold into the medium of cultured neurons 1 h after plating.

Treatment with Antibody, Enzymes, and Pharmacological Agents—Anti-MAG antibody, enzymes, and pharmacological agents were added to cultures 1 h after cell plating. None of the treatments resulted in any reduction in cell number or any change in average neurite outgrowth on control substrata (data not shown). The efficacy of PI-PLC, which cleaves GPI-anchored proteins including NgRs from cell surfaces (26), was confirmed by a reduction in immunostaining of a GPI-anchored protein, Thy-1 (27). The efficacy of sialidase, which cleaves MAG-binding terminal sialic acids from cell surfaces (28), and of P4 (29), which blocks glycosphingolipid biosynthesis (12), was confirmed by elimination of GD1a immunostaining (30). The inhibitory efficacy of TAT-Pep5 was confirmed by blocking pro-nerve growth factor-mediated apoptosis in hippocampal neurons, a p75-induced event (31).

Neurite Outgrowth Inhibition Assay—After 24–48 h (depending on the cell type, see above) cultures were washed with Dulbecco's phosphate-buffered saline, fixed overnight with 2% paraformaldehyde in Dulbecco's phosphate-buffered saline, and then permeabilized using 0.1% Triton X-100 in Dulbecco's phosphate-buffered saline. DRGNs and HNs were immunostained with anti-neuronal class III β-tubulin monoclonal antibody (TUJ1, 1:2000, Covance, Berkeley, CA) followed by Cy3-conjugated anti-mouse IgG (1:200, Jackson ImmunoResearch Laboratories, West Grove, PA). CGNs were immunostained with GAP43 polyclonal antibody (1:1000, AbCam, Cambridge, MA) followed by Cy3-conjugated goat anti-rabbit IgG (1:300, Jackson ImmunoResearch Laboratories) mixed with 300 nM 4′,6-diamidino-2-phenylindole (Invitrogen). After washing, multiple random fields were captured for image analysis using a Nikon TE300 epifluorescence microscope fitted with a Photometrics CoolSNAP HQ2 camera (Roper Scientific, Duluth, GA).

Neurite outgrowth from DRGNs and HNs was quantified using Metamorph image analysis (Universal Imaging Systems, Downington, PA). Relative pixel staining intensity was assigned, and cell bodies were automatically subtracted from the image based on their high staining intensity (*e.g.* Fig. 1). Neurites were then quantified as the number of pixels having the intensity of neurites. That value was divided by the number of cell bodies in the field. Neurite area per cell body for each condition was normalized to the control and expressed as relative neurite outgrowth.

CGNs on control substrata extend very fine axons[6] (32) that form a lacy network on the culture surface. In contrast, CGN axons on inhibitory substrata fasciculate (see Fig. 5) avoid the substratum and grow over each other. To differentiate individual axons from fasciculated axons we developed an image analysis protocol using NIS-Elements software (Nikon, Melville, NY). CGN cell bodies were identified by co-localization of anti-GAP43 and 4′,6-diamidino-2-phenylindole staining and subtracted from the image. Relative anti-GAP43 pixel staining intensity was assigned. Axons were quantified as the sum of the pixels having intensities representative of individual, unfasciculated axons. There was no significant difference in the average number of cells per field in the experimental and control conditions (data not shown).

For each experimental condition four to five random images from each of 4–10 independent wells from an average of three independent experiments were analyzed. Data are presented as the means ± S.E. Statistical *p* values were obtained using Student's *t* test.

RESULTS

MAG Inhibition of DRGN Neurite Outgrowth Is Primarily via NgR and Secondarily via Gangliosides—Postnatal DRGNs extended long neurites within 24 h when plated on control surfaces (Fig. 1). When the same cells were plated on wells adsorbed with extracted myelin proteins, neurite outgrowth was sharply diminished. A function-blocking anti-MAG antibody reversed 70% of the inhibition in this *in vitro* model. PI-PLC, which releases GPI-anchored proteins (such as NgRs) from cell surfaces (26), reversed inhibition >50%, whereas sialidase, which releases MAG-binding sialic acid residues, reversed inhibition ~20%. When used together, PI-PLC and sialidase reversed inhibition 71% to the same level as anti-MAG antibody. These data are consistent with an additive role of GPI-anchored proteins and sialoglycans in mediating MAG inhibition in DRGN.

Specific pharmacological agents were used to further distinguish the receptors associated with MAG-mediated inhibition of DRGN neurite outgrowth (Fig. 2). Consistent with the enzyme data, addition of NEP1–40, a competitive antagonist peptide that blocks the Nogo-66/MAG binding site on NgR (14, 17), resulted in ~50% reversal of myelin-mediated inhibition, whereas P4, which blocks glycosphingolipid biosynthesis including gangliosides (29, 33), resulted in ~35% reversal. A scrambled peptide control for NEP1–40 (17) neither altered control axon outgrowth nor reversed myelin-mediated inhibition (72 ± 10% inhibition without peptide, 73 ± 4% inhibition with control peptide). The inactive (*S*,*S*) enantiomer of P4 also was without effect. Added together, NEP1–40 and P4 reversed inhibition to the same level as anti-MAG antibody.

The quantitatively similar reversal of MAG inhibition of neurite outgrowth from DRGNs by PI-PLC and NEP1–40 implicates NgR as the primary receptor. Significant but quantitatively less reversal by sialidase and P4 implicates gangliosides as secondary receptors. The ability of the combined hydrolytic enzymes (or the combined inhibitors) to reverse inhibition to the same level as anti-MAG antibody suggests independent NgR and ganglioside pathways for MAG inhibition.

NgR has been reported to associate laterally in the plane of the axon membrane with the neurotrophin receptor $p75^{NTR}$, a

[6] The general term "neurite" is used to describe the thin extensions from DRGNs and HNs in cell culture. Extensions from cerebellar granule neurons are termed "axons" because morphological and immunohistochemical criteria identify early extending neurites from rodent CGNs as axons (32).

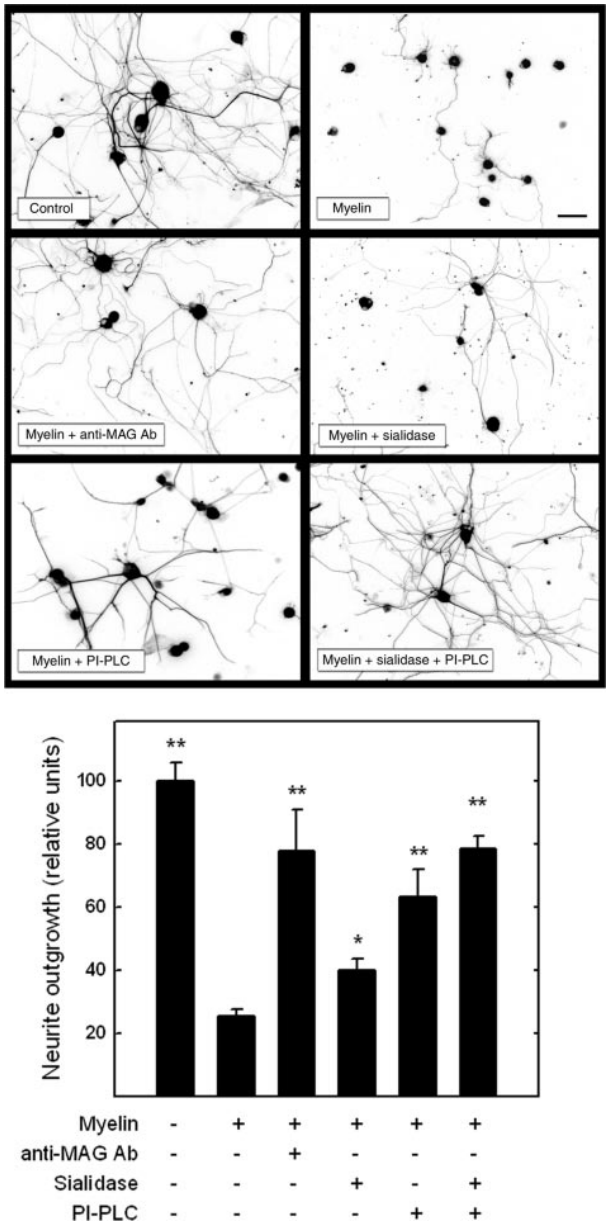

FIGURE 1. **MAG inhibition of neurite outgrowth from DRGNs is via both GPI-anchored proteins and sialoglycans.** DRGNs were plated on control surfaces or the same surfaces adsorbed with detergent-extracted myelin proteins (*Myelin*). As indicated, 1 h after plating, cultures were treated with 10 μg/ml anti-MAG mAb, 8 milliunits/ml sialidase, or 1 unit/ml PI-PLC. After 24 h, the cultures were fixed and stained with anti-tubulin mAb. Representative fluorescence micrographs are presented as reverse gray scale images to enhance clarity (*bar*, 50 μm). Neurite outgrowth (mean $\pm$ S.E.) was quantified using image analysis and normalized with respect to the control. *Symbols* indicate statistical comparison with myelin-inhibited neurite outgrowth: *, $p < 0.01$; **, $p < 0.001$. *Ab*, antibody.

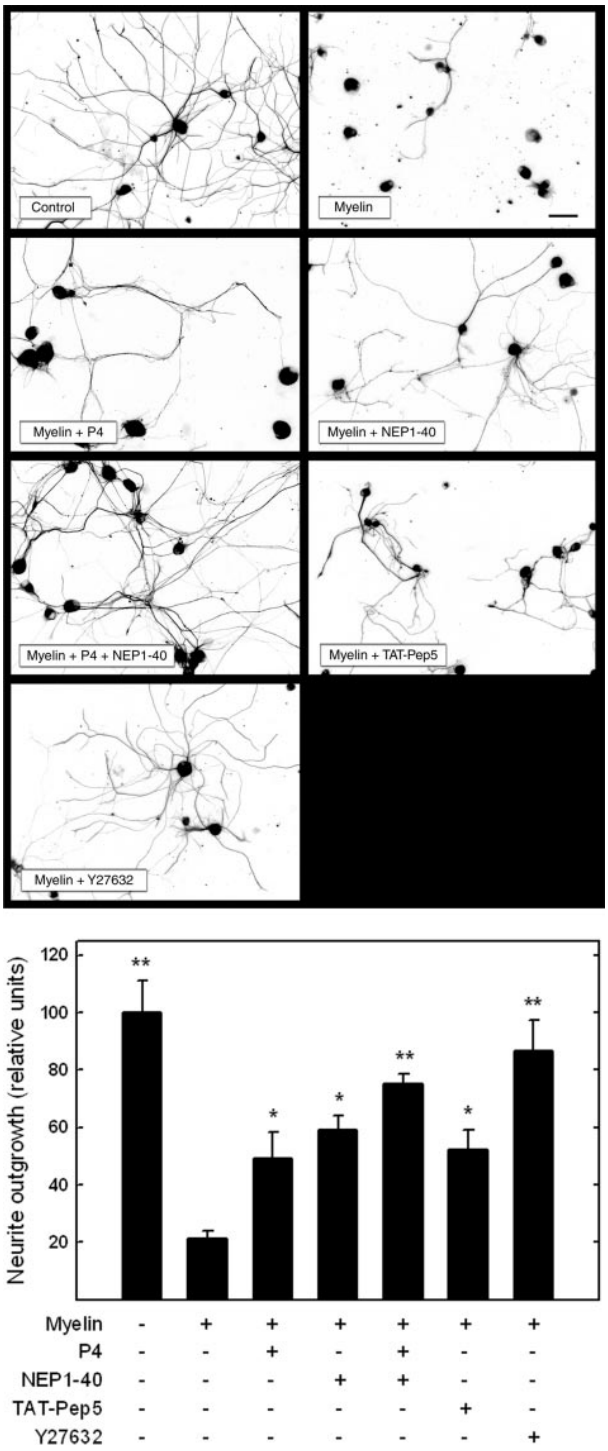

FIGURE 2. **MAG inhibition of neurite outgrowth from DRGNs is via both NgR and glycosphingolipids.** DRGNs were plated on control surfaces or the same surfaces adsorbed with detergent-extracted myelin proteins (*Myelin*). As indicated,1 h after plating, cultures were treated with 1 μM P4, 1 μM NEP1–40, 200 nM TAT-Pep5, or 10 μM Y-27632. After 24 h, the cultures were fixed and stained with anti-tubulin mAb. Representative fluorescence micrographs are presented as reverse gray scale images to enhance clarity (*bar*, 50 μm). Neurite outgrowth (mean $\pm$ S.E.) was quantified using image analysis and normalized with respect to the control. *Symbols* indicate statistical comparison with myelin-inhibited neurite outgrowth: *, $p < 0.01$; **, $p < 0.001$.

transmembrane protein proposed to transduce the NgR binding response from MAG, Nogo, and OMgp to the small GTPase RhoA (34–36). A cell-permeable peptide, TAT-Pep5, blocks the intracellular association of $p75^{NTR}$ with Rho GDP dissociation inhibitor, blocking its ability to activate RhoA (16). When added to DRGNs on myelin-adsorbed substratum, TAT-Pep5 reversed MAG-mediated inhibition ~40% (Fig. 2), whereas Y-27632 (37), which blocks Rho kinase (a downstream RhoA effector), reversed inhibition >80%. These data are consistent with $p75^{NTR}$ acting as a transducer for a portion of the inhibitory effect of MAG on DRGNs, whereas nearly all inhibition is via RhoA activation.

Inhibition of Neurite Outgrowth from DRGNs by the Soluble Extracellular Domain of Native MAG Is via NgR—MAG exists primarily as a transmembrane protein and is found on myelin membranes at sites of central nervous system injury (5). In addition, an endogenous protease cleaves a portion of MAG at the injury site, spontaneously releasing the entire extracellular domain, dMAG, which may diffuse to nearby axons and inhibit regeneration (38). dMAG is also spontaneously released from isolated purified myelin (39).

Because different physical forms of MAG may act via different receptors, we repeated the above experiments instead using dMAG to inhibit neurite outgrowth. dMAG was prepared by incubating purified myelin for 18–24 h in culture medium (8) and was separated from membrane-bound MAG by ultracentrifugation. Addition of dMAG to DRGN cultures inhibited neurite outgrowth (Fig. 3), and dMAG-mediated inhibition was largely reversed by anti-MAG mAb. PI-PLC and NEP1–40 independently and completely reversed dMAG-mediated inhibition, whereas sialidase and P4 had little or no effect when added independently or in combination with PI-PLC and NEP1–40. We conclude that, on DRGNs, soluble dMAG exerts its inhibitory effects via NgR, whereas substrate-adsorbed full-length MAG accesses both NgR and gangliosides to inhibit neurite outgrowth.

Neurite Outgrowth from DRGNs Plated on Myelin Extracts from Wild Type and MAG-null Mice Reveals NgR and Gangliosides as Dual MAG Receptors—Surfaces adsorbed with mild detergent extract from wild type mouse myelin robustly inhibited DRGN neurite outgrowth, whereas extracts from MAG-null mouse myelin had little inhibitory potency (Fig. 4). Addition of anti-MAG antibody reversed the inhibition by wild type myelin extract to the same level as MAG-null extract. Consistent with the findings using rat myelin extract, over half of the MAG-mediated inhibition was reversed by treatment with PI-PLC or with NEP1–40. A significant but smaller proportion of MAG-mediated inhibition was reversed by treatment with sialidase or P4. The combination of enzymes (PI-PLC and sialidase) or inhibitors (NEP1–40 and P4) completely reversed inhibition on wild type myelin extract to the level of MAG-null myelin extract (Fig. 4). These data confirm that the inhibition of neurite outgrowth from DRGNs by detergent extracts of myelin in the current *in vitro* model is primarily MAG-mediated and that DRGNs respond to full-length native MAG primarily via NgR and secondarily via gangliosides.

MAG Inhibition of Axon Outgrowth from Cerebellar Granule Neurons Is Exclusively via Gangliosides—CGNs extend a fine meshwork of axons when cultured for 48 h on control substrata (Figs. 5–8). In contrast, when cultured on surfaces adsorbed with myelin extract, the axons tend to fasciculate, leaving large areas of the substratum free of axons (*e.g.* Fig. 5, *Myelin*). Addition of anti-MAG antibody to CGNs cultured on myelin-adsorbed surfaces reversed much of the inhibition. Quantification via image analysis revealed 32% inhibition by myelin extract of which 60% was reversed by anti-MAG antibody (Fig. 5). Addition of sialidase reversed inhibition to the same level as anti-MAG antibody, whereas addition of PI-PLC had no effect whether added alone or in combination with sialidase. Consistent with the enzyme effects, addition of the glycosphingolipid inhibitor P4 reversed inhibition of axon outgrowth to the same level as anti-MAG antibody, whereas addition of NEP1–40 (alone or in combination with P4) had no effect (Fig. 6). Addition of TAT-Pep5 ($p75^{NTR}$ blocker) had no significant ability to reverse MAG-mediated inhibition, whereas Y-27632 (Rho kinase blocker) completely reversed inhibition.

Inhibition of CGN axon outgrowth by soluble dMAG was fully ganglioside-dependent; dMAG-mediated inhibition was equally reversed by addition of anti-MAG antibody, sialidase,

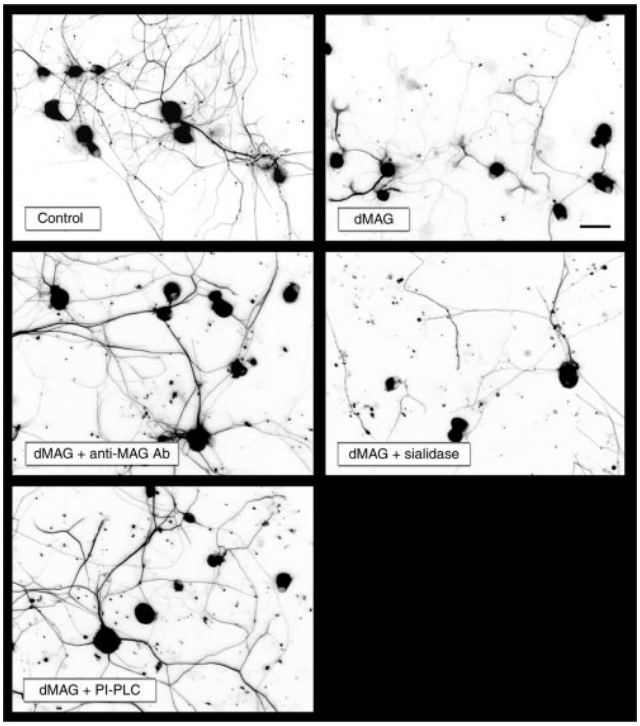

FIGURE 3. **Inhibition of neurite outgrowth from DRGNs by dMAG is predominantly via NgR.** DRGNs were plated on control surfaces. dMAG was added to the indicated cultures 1 h after plating. As indicated, cultures were treated at the same time with 10 μg/ml anti-MAG mAb, 8 milliunits/ml sialidase, 1 unit/ml PI-PLC, 1 μM P4, or 1 μM NEP1–40. After 24 h, the cultures were fixed and stained with anti-tubulin mAb. Representative fluorescence micrographs are presented as reverse gray scale images to enhance clarity (*bar*, 50 μm). Neurite outgrowth (mean $\pm$ S.E.) was quantified using image analysis and normalized with respect to the control. *Symbols* indicate statistical comparison with myelin-inhibited neurite outgrowth: *, $p < 0.01$; *ns*, not statistically significant. *Ab*, antibody.

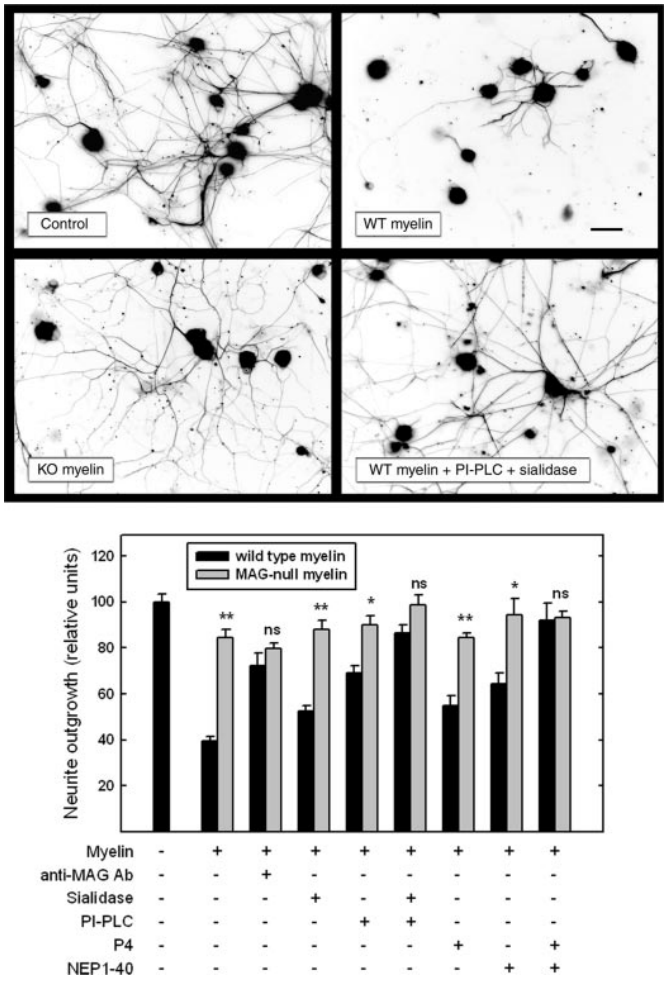

FIGURE 4. **Neurite outgrowth from DRGNs on substrata adsorbed with extracts of wild type and MAG-null mouse myelin demonstrates that MAG-mediated inhibition is via NgR and gangliosides.** Rat DRGNs were plated on control surfaces or the same surfaces adsorbed with detergent-extracted myelin proteins from wild type mouse brain (*WT*) or MAG-null mouse brain (*KO*). As indicated, cultures were treated 1 h after plating with 10 μg/ml anti-MAG mAb, 8 milliunits/ml sialidase, 1 unit/ml PI-PLC, 1 μM P4, or 1 μM NEP1–40. After 24 h, the cultures were fixed and stained with anti-tubulin mAb. Representative fluorescence micrographs are presented as reverse gray scale images to enhance clarity (*bar*, 50 μm). Neurite outgrowth (mean ± S.E.) was quantified using image analysis and normalized with respect to the control. *Symbols* indicate statistical comparison of identically treated wild type and MAG-null cultures: *, $p < 0.02$; **, $p < 0.001$; *ns*, not statistically significant. All treatments significantly reversed the inhibition due to wild type mouse myelin extract ($p < 0.01$). *Ab*, antibody.

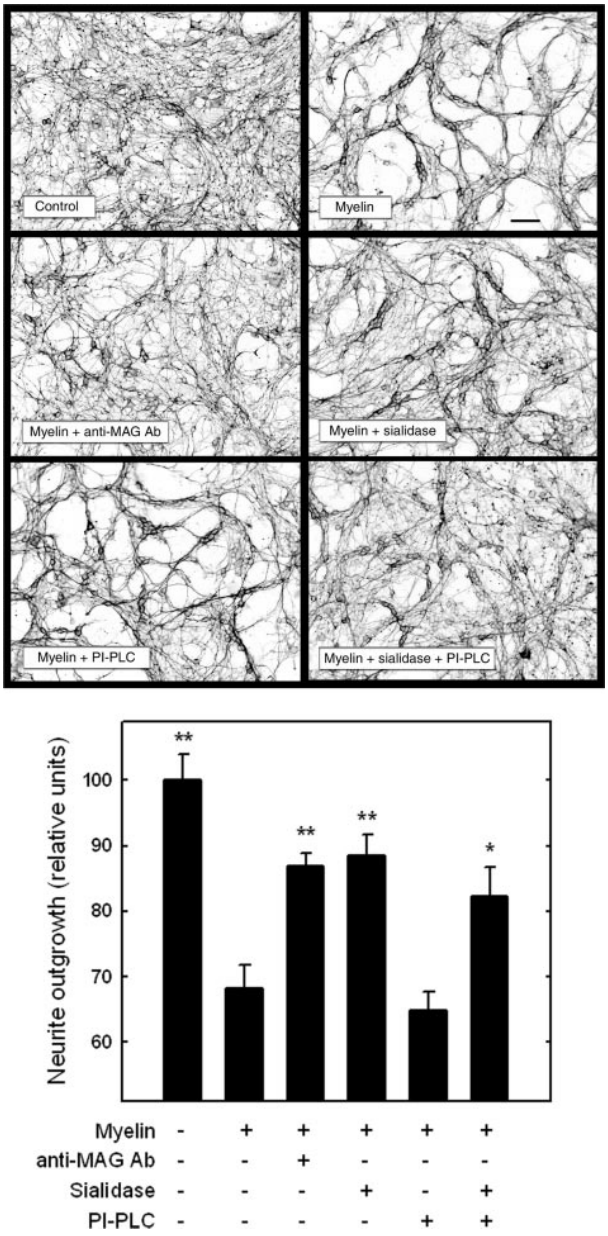

FIGURE 5. **MAG inhibition of axon outgrowth from CGNs is via sialoglycans.** CGNs were plated on control surfaces or the same surfaces adsorbed with detergent-extracted myelin proteins (*Myelin*). As indicated, 1 h after plating, cultures were treated with 10 μg/ml anti-MAG mAb, 8 milliunits/ml sialidase, or 1 unit/ml PI-PLC. After 48 h, the cultures were fixed and stained with anti-GAP43 antibody. Representative fluorescence micrographs are presented as reverse gray scale images to enhance clarity (*bar*, 50 μm). Axon outgrowth (mean ± S.E.) was quantified using image analysis and normalized with respect to the control. *Symbols* indicate statistical comparison with myelin-inhibited axon outgrowth: *, $p < 0.01$; **, $p < 0.001$. *Ab*, antibody.

or P4 (Fig. 7). Addition of PI-PLC or NEP1–40 had no effect on dMAG inhibition.

Surfaces adsorbed with mild detergent extract of wild type mouse myelin significantly inhibited CGN axon outgrowth, whereas extract of MAG-null mouse myelin had no inhibitory effect (Fig. 8). Independent treatment with sialidase or P4 completely reversed wild type MAG inhibition as did anti-MAG antibody ($p < 0.005$). Treatment with PI-PLC or NEP1–40 had no effect on MAG inhibition. CGN axon outgrowth on surfaces adsorbed with extract from MAG-null myelin was indistinguishable from outgrowth on control surfaces and was unaffected by addition of enzymes or pharmacological agents (Fig. 8). The results from Figs. 5–8 indicate that gangliosides are the exclusive receptors for MAG-mediated inhibition of axon outgrowth from CGNs.

MAG Inhibition of Neurite Outgrowth from Hippocampal Neurons Is Primarily via Gangliosides—On control substrata, HNs extend long branched neurites with fine arborizations (Figs. 9–11). On substrata adsorbed with mild detergent extract of myelin, neurites were fewer in number and less branched; image analysis indicated a 35% reduction in total neurite area per cell of which 70% was reversed by

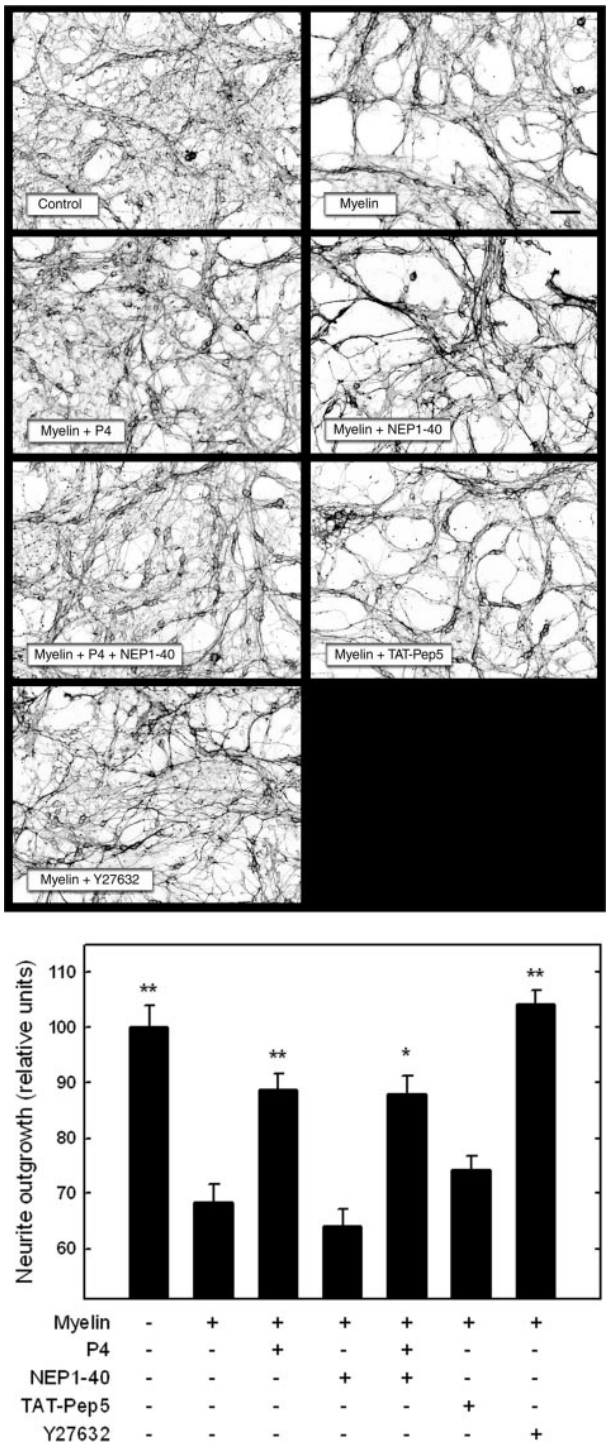

FIGURE 6. **MAG inhibition of axon outgrowth from CGNs is via glycosphingolipids.** CGNs were plated on control surfaces or the same surfaces adsorbed with detergent-extracted myelin proteins (*Myelin*). As indicated, 1 h after plating, cultures were treated with 1 μM P4, 1 μM NEP1–40, 100 nM TAT-Pep5, or 5 μM Y-27632. After 48 h, the cultures were fixed and stained with anti-GAP43 antibody. Representative fluorescence micrographs are presented as reverse gray scale images to enhance clarity (*bar*, 50 μm). Axon outgrowth (mean $\pm$ S.E.) was quantified using image analysis and normalized with respect to the control. *Symbols* indicate statistical comparison with myelin-inhibited axon outgrowth: *, $p < 0.01$; **, $p < 0.001$.

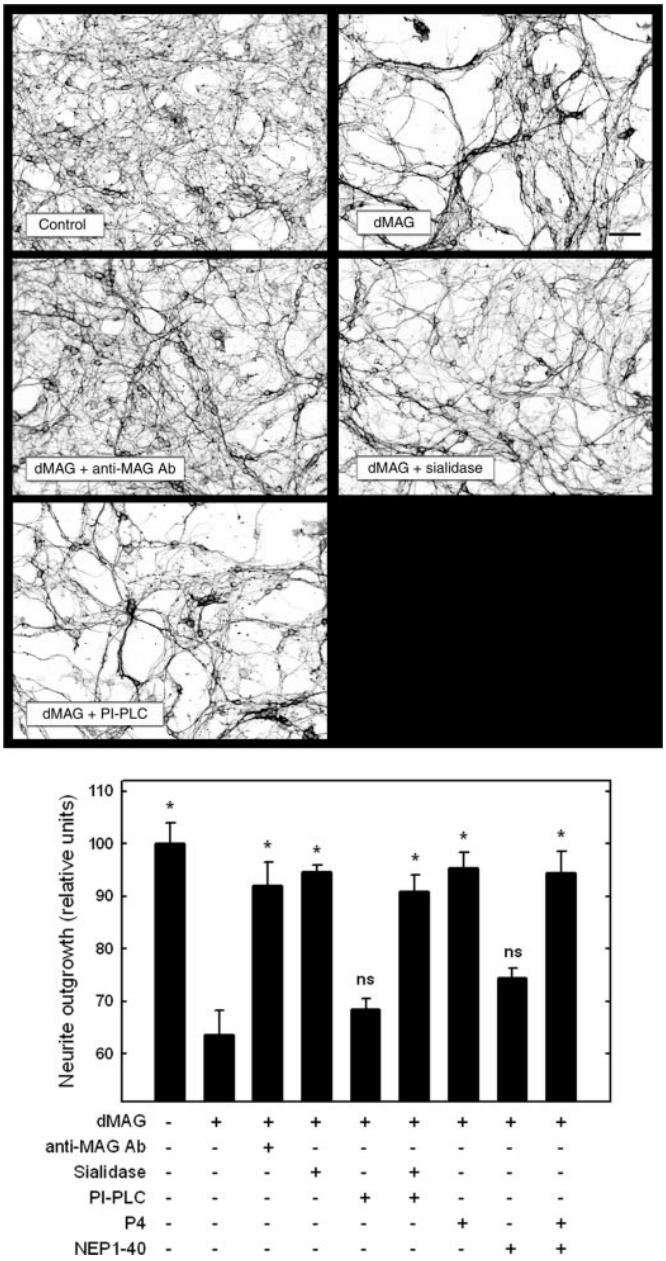

FIGURE 7. **Inhibition of axon outgrowth from CGNs by dMAG is via gangliosides.** CGNs were plated on control surfaces. dMAG was added to the indicated cultures 1 h after plating. As indicated, cultures were treated at the same time with 10 μg/ml anti-MAG antibody, 8 milliunits/ml sialidase, 1 unit/ml PI-PLC, 1 μM P4, or 1 μM NEP1–40. After 48 h, the cultures were fixed and stained with anti-GAP43 antibody. Representative fluorescence micrographs are presented as reverse gray scale images to enhance clarity (*bar*, 50 μm). Axon outgrowth (mean $\pm$ S.E.) was quantified using image analysis and normalized with respect to the control. *Symbols* indicate statistical comparison with myelin-inhibited axon outgrowth: *, $p < 0.005$; *ns*, not statistically significant. *Ab*, antibody.

monoclonal anti-MAG mAb (Fig. 9). Addition of sialidase reversed inhibition 60%, whereas PI-PLC reversed inhibition 30% (Fig. 9). Surprisingly combined enzyme treatment was equivalent to sialidase treatment alone. Consistent with these results, inhibition was reversed 73% by addition of P4 and 30% by addition of NEP1–40, and the combination did not enhance reversal over P4 (Fig. 10). These data suggest that a portion of the inhibition is both NgR- and ganglioside-dependent, whereas a portion is exclusively ganglioside-dependent. Addition of TAT-Pep5 resulted in reversal similar to that by PI-PLC or NEP1–40, whereas treatment with Rho

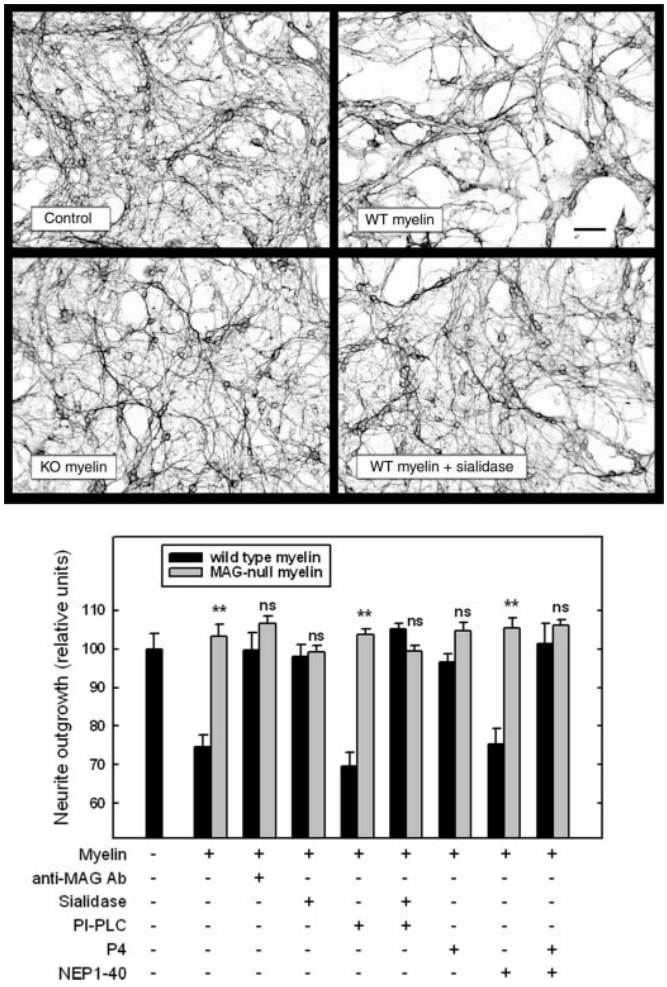

FIGURE 8. **Axon outgrowth from CGNs on substrata adsorbed with extracts of wild type and MAG-null mouse myelin demonstrates that MAG-mediated inhibition is via gangliosides.** Rat CGNs were plated on control surfaces or the same surfaces adsorbed with detergent-extracted myelin proteins from wild type mouse brain (*WT*) or MAG-null mouse brain (*KO*). As indicated, cultures were treated 1 h after plating with 10 μg/ml anti-MAG antibody, 8 milliunits/ml sialidase, 1 unit/ml PI-PLC, 1 μM P4, or 1 μM NEP1–40. After 48 h, the cultures were fixed and stained with anti-GAP43 antibody, and axon outgrowth was quantified as described in the text. Representative fluorescence micrographs are presented as reverse gray scale images to enhance clarity (*bar*, 50 μm). Axon outgrowth (mean ± S.E.) was quantified using image analysis and normalized with respect to the control. *Symbols* indicate statistical comparison of identically treated wild type and MAG-null cultures: **, $p < 0.001$; *ns*, not statistically significant.

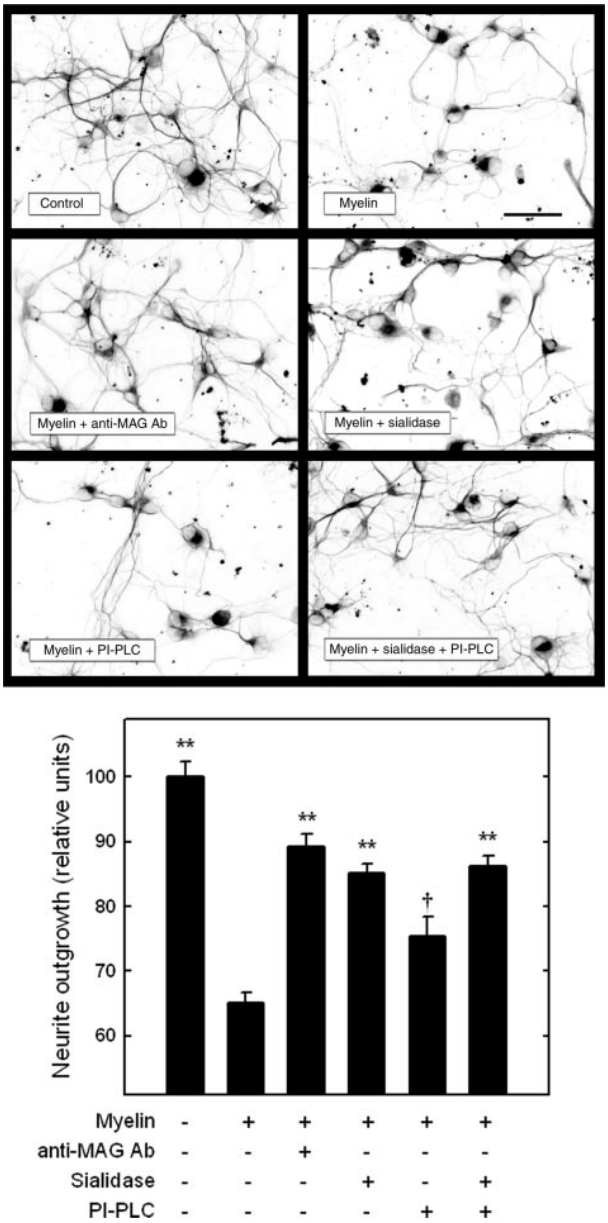

FIGURE 9. **MAG inhibition of neurite outgrowth from HNs is primarily via sialoglycans.** HNs were plated on control surfaces or the same surfaces adsorbed with detergent-extracted myelin proteins (*Myelin*). As indicated, 1 h after plating, cultures were treated with 10 μg/ml anti-MAG mAb, 8 milliunits/ml sialidase, or 250 milliunits/ml PI-PLC. After 48 h, the cultures were fixed and stained with anti-tubulin mAb. Representative fluorescence micrographs are presented as reverse gray scale images to enhance clarity (*bar*, 100 μm). Neurite outgrowth (mean ± S.E.) was quantified using image analysis and normalized with respect to the control. *Symbols* indicate statistical comparison with myelin-inhibited neurite outgrowth: †, $p < 0.02$; **, $p < 0.001$. *Ab*, antibody.

kinase inhibitor resulted in reversal similar to that by sialidase or P4 (or combined treatments).

Comparison of HN neurite outgrowth on control surfaces with that on surfaces adsorbed with extracts from wild type and MAG-null mouse myelin revealed that 62% of the myelin inhibition in this *in vitro* model was MAG-mediated (Fig. 11). Independent treatment of HNs cultured on wild type myelin extract with sialidase or P4 reversed inhibition to the level of MAG-null mouse myelin as did treatment with anti-MAG antibody ($p < 0.001$). Addition of PI-PLC ($p = 0.15$) or NEP1–40 ($p < 0.02$) resulted in minimal reversal and did not significantly enhance reversal when added to sialidase and P4, respectively. Axon outgrowth from HNs on MAG-null myelin was unaffected by treatment with the individual enzymes or pharmacological agents. Our results indicate that MAG inhibition of neurite outgrowth from HNs is predominantly ganglioside-dependent, although a portion of the myelin-mediated inhibition appears to involve NgR and $p75^{NTR}$.

DISCUSSION

MAG is a multifunctional myelin protein that enhances axon-myelin stability, regulates the axon cytoskeleton, and stabilizes the distribution of molecules at nodes of Ranvier (5, 40–43). In addition to its physiological functions, MAG is

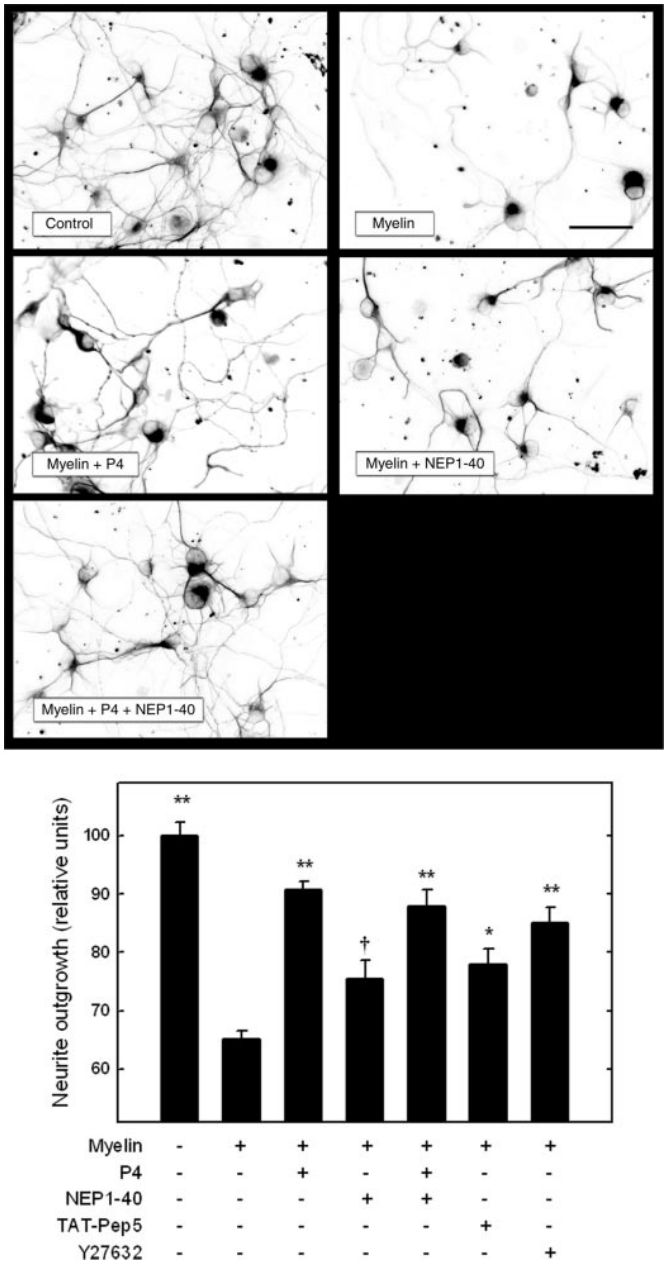

FIGURE 10. **MAG inhibition of neurite outgrowth from HNs is primarily via glycosphingolipids.** HNs were plated on control surfaces or the same surfaces adsorbed with detergent-extracted myelin proteins (*Myelin*). As indicated, 1 h after plating, cultures were treated with 1 μM P4, 1 μM NEP1–40, 100 nM TAT-Pep5, or 5 μM Y-27632. After 48 h, the cultures were fixed and stained with anti-tubulin mAb. Representative fluorescence micrographs are presented as reverse gray scale images to enhance clarity (*bar*, 100 μm). Neurite outgrowth (mean ± S.E.) was quantified using image analysis and normalized with respect to the control. *Symbols* indicate statistical comparison with myelin-inhibited neurite outgrowth: †, $p < 0.02$; *, $p < 0.01$; **, $p < 0.001$.

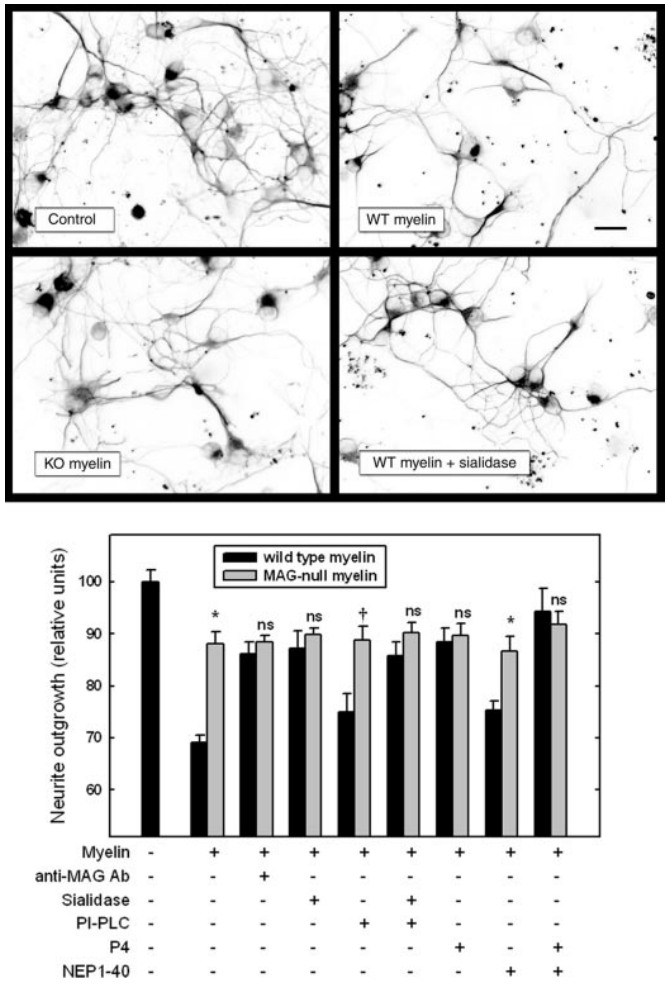

FIGURE 11. **Neurite outgrowth from HNs on substrata adsorbed with extracts of wild type and MAG-null mouse myelin demonstrates that MAG-mediated inhibition is primarily via gangliosides.** Rat HNs were plated on control surfaces or the same surfaces adsorbed with detergent-extracted myelin proteins from wild type mouse brain (*WT*) or MAG-null mouse brain (*KO*). As indicated, cultures were treated 1 h after plating with 10 μg/ml anti-MAG mAb, 8 milliunits/ml sialidase, 250 milliunits/ml PI-PLC, 1 μM P4, or 1 μM NEP1–40. After 48 h, the cultures were fixed and stained with anti-tubulin mAb. Representative fluorescence micrographs are presented as reverse gray scale images to enhance clarity (*bar*, 100 μm). Neurite outgrowth (mean ± S.E.) was quantified using image analysis and normalized with respect to the control. *Symbols* indicate statistical comparison of identically treated wild type and MAG-null cultures: †, $p < 0.05$; *, $p < 0.01$; *ns*, not statistically significant.

among a group of molecules that inhibit axon regeneration at sites of injury thereby limiting functional recovery (1, 2). These ARIs include MAG, Nogo, and OMgp on residual myelin and chondroitin sulfate proteoglycans on the astrocytic scar. Destruction of or blocking ARIs may enhance axon regeneration and functional recovery (3). Identification of the molecular components of each ARI signaling system provides potential targets for therapeutic intervention.

Our data indicate that there are dual receptors that independently mediate MAG inhibition. Using native MAG extracted from rat or mouse myelin, or a soluble fragment of native MAG, and using a set of enzymatic and pharmacological agents to modulate potential MAG receptors, we found that different nerve cell types use different MAG receptors (Table 1). The clearest example of alternative receptors was in the response of DRGNs and CGNs to dMAG. dMAG acts exclusively via a PI-PLC- and NEP1–40-sensitive mechanism in DRGNs and exclusively via a sialidase- and P4-sensitive mechanism in CGNs (Figs. 3 and 7). The near complete lack of overlap in receptor utility in these experiments implies the independent ability of NgRs and gangliosides to mediate MAG inhibition and argues against a requirement for functional association between the NgR pathway and the ganglioside pathway.

TABLE 1
Enzymes and agents used in these studies

Agent	Target	Reversal of MAG inhibition[a]
Sialidase	Terminal sialic acids	CGN, HN, (DRGN)
PI-PLC	GPI-anchored proteins	DRGN, (HN)
P4	Glycosphingolipid biosynthesis	CGN, HN, (DRGN)
NEP1–40	NgR1 (NgR2?)	DRGN, (HN)
TAT-Pep5	$p75^{NTR}$	DRGN, (HN)
Y-27632	Rho kinase (ROCK)	DRGN, CGN, HN

[a] Nerve cell types are listed if the associated treatment resulted in statistically significant reversal of MAG inhibition of neurite outgrowth. Parentheses are used to designate neuronal cell types in which the associated treatment resulted in statistically significant but modest quantitative reversal (<40%).

The dual independent receptor hypothesis is consistent with our other findings. The additive ability of PI-PLC and sialidase (or P4 and NEP1–40) to reverse MAG inhibition of DRGN neurite outgrowth to levels equivalent to either anti-MAG or MAG-null controls (Figs. 1, 2, and 4) is consistent with independent pathways that act within cells or cell populations to restrict DRGN neurite outgrowth. In CGNs, sialidase or P4 reversal of axon outgrowth inhibition by MAG and the lack of significant reversal by PI-PLC or NEP-40 are consistent with a ganglioside-dependent pathway that is wholly independent of the NgR-dependent pathway.

The quantitatively similar reversal of MAG inhibition by sialidase and P4 in three different nerve cell types implicate gangliosides (sialoglycosphingolipids) rather than sialoglycoproteins as functional MAG receptors (12). Gangliosides are the major sialoglycans in the nervous system (44); the major MAG-binding gangliosides, GD1a and GT1b, are among the most abundant and widely distributed (45).

PI-PLC and the peptide inhibitor NEP1–40 led to similar quantitative reversal of MAG inhibition of neurite outgrowth from DRGNs and HNs. As GPI-anchored proteins, NgRs are sensitive to PI-PLC release (15, 26). NEP1–40, a sequence derived from Nogo-66, is a competitive antagonist of Nogo-NgR1 binding (17). Although NEP1–40 had not been known to block MAG-NgR binding (13), MAG and Nogo compete for a similar binding site on NgR (14, 46). We conclude that NEP1–40 and PI-PLC are acting at the same MAG receptor sites (NgR1 and/or NgR2) on DRGNs and HNs. An alternative hypothesis is that a portion of inhibition in our assays is due to extracted and adsorbed Nogo. Although this cannot be excluded in all cases, it is unlikely to account, for instance, for the nearly complete reversal of dMAG inhibition of DRGN neurite outgrowth by addition of either anti-MAG antibody or NEP1–40 (Fig. 4). Likewise addition of anti-MAG antibody or a combination of P4 and NEP1–40 reversed inhibition of DRGN neurite outgrowth on wild type mouse myelin extract to the same level as that on MAG-null mouse extract, implicating MAG as the primary inhibitor in our *in vitro* assay system (Fig. 4) and NEP1–40 as an effective blocker of MAG.

Both NgR1 and NgR2 bind MAG and mediate its inhibition (13–15, 46). Because the relative selectivity of NEP1–40 for NgR1 and NgR2 has not been detailed, further experiments will be needed to identify which is operative in DRGNs and HNs.

Prior reports identifying either gangliosides or NgRs as functional receptors for MAG used a variety of nerve cell types *in vitro*, a variety of MAG sources (native and recombinant), and different measures of neurite outgrowth. Although our data reconcile some of these apparently conflicting findings, other discrepancies have yet to be resolved. In this light, it may be relevant that MAG is heavily glycosylated and that expression of recombinant forms in ectopic cells may result in sialylated glycoforms that bind to the glycan binding site of MAG and alter its binding. This hypothesis is supported by data showing that pretreatment of MAG-expressing CHO or COS cells with sialidase enhanced their ability to bind gangliosides (47). Because some nerve cell types (or populations) display dual MAG receptor pathways (*e.g.* DRGNs and HNs), one can envision that the nature of the MAG receptor used may depend on the glycosylation state of MAG or adjacent sialoglycans in experimental systems and perhaps *in vivo*.

ARIs bind to axon or growth cone receptors, initiating a signal cascade that results in RhoA activation, engagement of Rho effectors (*e.g.* Rho kinase), control of actin polymerization, and inhibition of axon outgrowth (1, 2). The molecules that link MAG-receptor binding to RhoA activation have not been fully elucidated. It has been proposed that MAG-NgR1 binds to the transmembrane neurotrophin receptor $p75^{NTR}$ (or alternatively the related protein TROY) in complex with Lingo-1 to engage Rho GDP dissociation inhibitor and activate RhoA (34–36, 48–50). In each of the nerve cell systems tested, we found that Y-27632, an inhibitor of Rho kinase (37), was effective in reversing MAG-mediated neurite outgrowth inhibition (Figs. 2, 6, and 10). Because MAG accessed different receptors in the different nerve cell types, we conclude that RhoA is downstream of each receptor. In contrast, a $p75^{NTR}$-blocking peptide, TAT-Pep5 (16), quantitatively tracked with PI-PLC and NEP1–40 in its ability to reverse MAG inhibition, having no effect on inhibited CGNs but partially reversing MAG inhibition of DRGNs and HNs (Table 1). We conclude that $p75^{NTR}$ is not a required transducer for MAG-ganglioside-mediated inhibition. The quantitatively similar effects of the inhibitors of p75 and NgR are consistent with their functional association.

Previous studies reported a physical interaction between gangliosides and $p75^{NTR}$ as part of an NgR-mediated signaling pathway in response to MAG-Fc-mediated inhibition of axon outgrowth from CGNs (35, 51). Our data, in contrast, indicate that ganglioside-mediated MAG inhibition of CGNs is independent of NgR or $p75^{NTR}$ (Figs. 5–8). The basis for this difference has yet to be determined, although different physical forms of MAG (native and MAG-Fc) and different axon outgrowth measures were used.

In our HN studies, PI-PLC modestly reversed MAG inhibition, sialidase robustly reversed inhibition, and the two were not additive (Figs. 9 and 11). Similarly partial reversal by NEP1–40 was not additive with more robust reversal by P4. TAT-Pep5 reversal was equivalent to that of PI-PLC/NEP1–40. These data are consistent with a portion of the ganglioside-mediated MAG inhibition being associated with NgR/$p75^{NTR}$ in HNs. However, given the modest amount of reversal by PI-PLC/NEP1–40/TAT-Pep5 in HNs, we cannot rule out a minor inhibitory role of non-MAG inhibitors on our *in vitro* inhibitory substrate.

A model that fits our data is presented in Fig. 12. We propose that there are at least two independent pathways for MAG inhi-

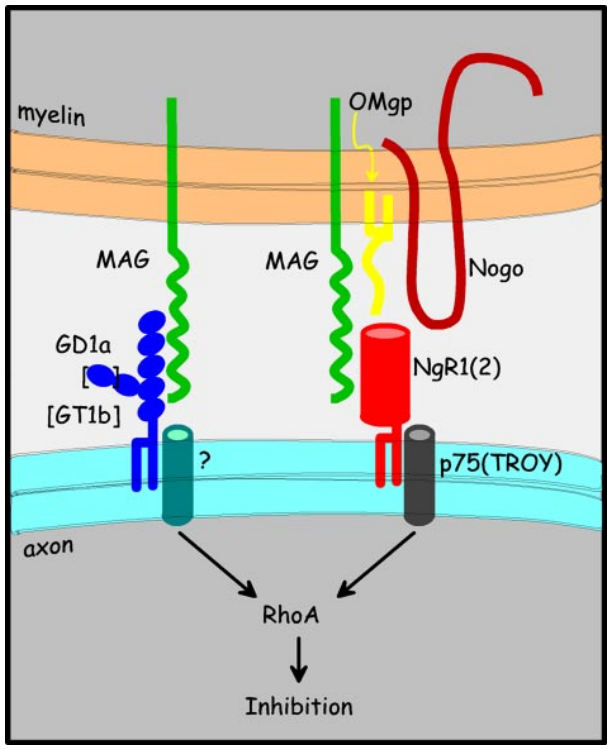

FIGURE 12. **Dual receptor model of MAG-mediated inhibition of axon regeneration.** MAG is proposed to bind independently to gangliosides GD1a/GT1b and Nogo receptors NgR1/NgR2. Nogo receptors may associate with $p75^{NTR}$ (or structurally related TROY) to transduce binding, through multiple steps, to RhoA activation, whereas the molecules that transduce MAG-ganglioside binding have yet to be fully determined. Cross-talk between pathways or combinations of the two pathways (*e.g.* ganglioside association with $p75^{NTR}$ in some cells (35)) are not excluded but are left off the model for clarity.

bition of neurite outgrowth, one via binding to gangliosides and a second via binding to NgRs. Both pathways link to RhoA activation. Published data support a role for $p75^{NTR}$ as a signal transducer for the NgR pathway. Our data using DRGNs and HNs are consistent with this pathway. MAG inhibition via gangliosides in CGNs did not appear to require NgR or $p75^{NTR}$ and therefore must signal via another transducer.

A recent report further supports the model in Fig. 12 (52). Sialidase modestly but significantly attenuated axon outgrowth inhibition when CGNs were cultured on Chinese hamster ovary cells ectopically expressing MAG (MAG-CHO cells) but failed to attenuate inhibition of retinal ganglion neurons on the same MAG-expressing cells. Notably MAG inhibition of neurite outgrowth from retinal neurons obtained from mice lacking NgR1 was partially reversed by sialidase. Furthermore CGNs and retinal neurons from mice lacking $p75^{NTR}$ or TROY remained sensitive to MAG-CHO inhibition. These data are fully consistent with at least two MAG receptors, one of which is sialidase-sensitive. The reason for more robust reversal of inhibition by sialidase and modifiers of NgRs in our study may be related to the physical nature of the inhibitor used (native MAG *versus* MAG-CHO) or differences in neurite outgrowth measures.

The existence of dual (or multiple) independent receptors that mediate MAG inhibition of axon outgrowth from different neuronal cell types implies that a single receptor-targeted therapy may not be uniformly successful in enhancing therapeutic recovery from nerve injury or disease (53). Quantifying the relative roles of the different MAG receptors on different axons may provide more accurate insights into the potential and limitations of different therapeutic interventions. Identifying the associated downstream transducing molecules and their points of convergence may also help in the development of therapeutics to enhance recovery from traumatic nerve injury and disease.

Acknowledgments—We thank Dr. Garry Taylor, University of St. Andrews, for generously supplying the sialidase expression vector; Dr. Melitta Schachner, Hamburg University, for the anti-MAG hybridoma; and Dr. David Meyers, The Johns Hopkins University, for synthesis of P4.

REFERENCES

1. Sandvig, A., Berry, M., Barrett, L. B., Butt, A., and Logan, A. (2004) *Glia* **46,** 225–251
2. Yiu, G., and He, Z. (2006) *Nat. Rev. Neurosci.* **7,** 617–627
3. David, S., and Lacroix, S. (2003) *Annu. Rev. Neurosci.* **26,** 411–440
4. Spencer, T., Domeniconi, M., Cao, Z., and Filbin, M. T. (2003) *Curr. Opin. Neurobiol.* **13,** 133–139
5. Quarles, R. H. (2007) *J. Neurochem.* **100,** 1431–1448
6. McKerracher, L., David, S., Jackson, D. L., Kottis, V., Dunn, R. J., and Braun, P. E. (1994) *Neuron* **13,** 805–811
7. Mukhopadhyay, G., Doherty, P., Walsh, F. S., Crocker, P. R., and Filbin, M. T. (1994) *Neuron* **13,** 757–767
8. Tang, S., Woodhall, R. W., Shen, Y. J., DeBellard, M. E., Saffell, J. L., Doherty, P., Walsh, F. S., and Filbin, M. T. (1997) *Mol. Cell. Neurosci.* **9,** 333–346
9. Lehmann, M., Fournier, A., Selles-Navarro, I., Dergham, P., Sebok, A., Leclerc, N., Tigyi, G., and McKerracher, L. (1999) *J. Neurosci.* **19,** 7537–7547
10. Varki, A., and Angata, T. (2006) *Glycobiology* **16,** 1R–27R
11. Yang, L. J. S., Zeller, C. B., Shaper, N. L., Kiso, M., Hasegawa, A., Shapiro, R. E., and Schnaar, R. L. (1996) *Proc. Natl. Acad. Sci. U. S. A.* **93,** 814–818
12. Vyas, A. A., Patel, H. V., Fromholt, S. E., Heffer-Lauc, M., Vyas, K. A., Dang, J., Schachner, M., and Schnaar, R. L. (2002) *Proc. Natl. Acad. Sci. U. S. A.* **99,** 8412–8417
13. Liu, B. P., Fournier, A., GrandPre, T., and Strittmatter, S. M. (2002) *Science* **297,** 1190–1193
14. Domeniconi, M., Cao, Z., Spencer, T., Sivasankaran, R., Wang, K., Nikulina, E., Kimura, N., Cai, H., Deng, K., Gao, Y., He, Z., and Filbin, M. (2002) *Neuron* **35,** 283–290
15. Venkatesh, K., Chivatakarn, O., Lee, H., Joshi, P. S., Kantor, D. B., Newman, B. A., Mage, R., Rader, C., and Giger, R. J. (2005) *J. Neurosci.* **25,** 808–822
16. Yamashita, T., and Tohyama, M. (2003) *Nat. Neurosci.* **6,** 461–467
17. GrandPre, T., Li, S., and Strittmatter, S. M. (2002) *Nature* **417,** 547–551
18. Moustafa, I., Connaris, H., Taylor, M., Zaitsev, V., Wilson, J. C., Kiefel, M. J., von Itzstein, M., and Taylor, G. (2004) *J. Biol. Chem.* **279,** 40819–40826
19. Poltorak, M., Sadoul, R., Keilhauer, G., Landa, C., Fahrig, T., and Schachner, M. (1987) *J. Cell Biol.* **105,** 1893–1899
20. Li, W. W., Walus, L., Rabacchi, S. A., Jirik, A., Chang, E., Schauer, J., Zheng, B. H., Benedetti, N. J., Liu, B. P., Choi, E., Worley, D., Silvian, L., Mo, W. J., Mullen, C., Yang, W. X., Strittmatter, S. M., Sah, D. W. Y., Pepinsky, B., and Lee, D. H. S. (2004) *J. Biol. Chem.* **279,** 43780–43788
21. Hatten, M. E. (1985) *J. Cell Biol.* **100,** 384–396
22. Vyas, K. A., Patel, H. V., Vyas, A. A., and Schnaar, R. L. (2001) *Biol. Chem.* **382,** 241–250
23. Brewer, G. J. (1997) *J. Neurosci. Methods* **71,** 143–155
24. Norton, W. T., and Poduslo, S. E. (1973) *J. Neurochem.* **21,** 749–757
25. Pan, B., Fromholt, S. E., Hess, E. J., Crawford, T. O., Griffin, J. W., Sheikh, K. A., and Schnaar, R. L. (2005) *Exp. Neurol.* **195,** 208–217

26. Fournier, A. E., GrandPre, T., and Strittmatter, S. M. (2001) *Nature* **409,** 341–346
27. Heffer-Lauc, M., Lauc, G., Nimrichter, L., Fromholt, S. E., and Schnaar, R. L. (2005) *Biochim. Biophys. Acta* **1686,** 200–208
28. Kelm, S., Pelz, A., Schauer, R., Filbin, M. T., Song, T., de Bellard, M. E., Schnaar, R. L., Mahoney, J. A., Hartnell, A., Bradfield, P., and Crocker, P. R. (1994) *Curr. Biol.* **4,** 965–972
29. Abe, A., Radin, N. S., Shayman, J. A., Wotring, L. L., Zipkin, R. E., Sivakumar, R., Ruggieri, J. M., Carson, K. G., and Ganem, B. (1995) *J. Lipid Res.* **36,** 611–621
30. Lunn, M. P., Johnson, L. A., Fromholt, S. E., Itonori, S., Huang, J., Vyas, A. A., Hildreth, J. E., Griffin, J. W., Schnaar, R. L., and Sheikh, K. A. (2000) *J. Neurochem.* **75,** 404–412
31. Lee, R., Kermani, P., Teng, K. K., and Hempstead, B. L. (2001) *Science* **294,** 1945–1948
32. Powell, S. K., Rivas, R. J., Rodriguez-Boulan, E., and Hatten, M. E. (1997) *J. Neurobiol.* **32,** 223–236
33. Li, R., Kong, Y., and Ladisch, S. (1998) *Glycobiology* **8,** 597–603
34. Wang, K. C., Kim, J. A., Sivasankaran, R., Segal, R., and He, Z. (2002) *Nature* **420,** 74–78
35. Yamashita, T., Higuchi, H., and Tohyama, M. (2002) *J. Cell Biol.* **157,** 565–570
36. Wong, S. T., Henley, J. R., Kanning, K. C., Huang, K. H., Bothwell, M., and Poo, M. M. (2002) *Nat. Neurosci.* **5,** 1302–1308
37. Uehata, M., Ishizaki, T., Satoh, H., Ono, T., Kawahara, T., Morishita, T., Tamakawa, H., Yamagami, K., Inui, J., Maekawa, M., and Narumiya, S. (1997) *Nature* **389,** 990–994
38. Tang, S., Qiu, J., Nikulina, E., and Filbin, M. T. (2001) *Mol. Cell. Neurosci.* **18,** 259–269
39. Sato, S., Quarles, R. H., Brady, R. O., and Tourtellotte, W. W. (1984) *Ann. Neurol.* **15,** 264–267
40. Fruttiger, M., Montag, D., Schachner, M., and Martini, R. (1995) *Eur. J. Neurosci.* **7,** 511–515
41. Yin, X., Crawford, T. O., Griffin, J. W., Tu, P., Lee, V. M., Li, C., Roder, J., and Trapp, B. D. (1998) *J. Neurosci.* **18,** 1953–1962
42. Marcus, J., Dupree, J. L., and Popko, B. (2002) *J. Cell Biol.* **156,** 567–577
43. Filbin, M. T. (2003) *Nat. Rev. Neurosci.* **4,** 703–713
44. Schnaar, R. L. (2004) *Arch. Biochem. Biophys.* **426,** 163–172
45. Tettamanti, G., Bonali, F., Marchesini, S., and Zambotti, V. (1973) *Biochim. Biophys. Acta* **296,** 160–170
46. Lauren, J., Hu, F., Chin, J., Liao, J., Airaksinen, M. S., and Strittmatter, S. M. (2007) *J. Biol. Chem.* **282,** 5715–5725
47. Collins, B. E., Yang, L. J. S., Mukhopadhyay, G., Filbin, M. T., Kiso, M., Hasegawa, A., and Schnaar, R. L. (1997) *J. Biol. Chem.* **272,** 1248–1255
48. Mi, S., Lee, X., Shao, Z. H., Thill, G., Ji, B. X., Relton, J., Levesque, M., Allaire, N., Perrin, S., Sands, B., Crowell, T., Cate, R. L., Mccoy, J. M., and Pepinsky, R. B. (2004) *Nat. Neurosci.* **7,** 221–228
49. Park, J. B., Yiu, G., Kaneko, S., Wang, J., Chang, J. F., and He, Z. G. (2005) *Neuron* **45,** 345–351
50. Shao, Z., Browning, J. L., Lee, X., Scott, M. L., Shulga-Morskaya, S., Allaire, N., Thill, G., Levesque, M., Sah, D., Mccoy, J. M., Murray, B., Jung, V., Pepinsky, R. B., and Mi, S. (2005) *Neuron* **45,** 353–359
51. Fujitani, M., Kawai, H., Proia, R. L., Kashiwagi, A., Yasuda, H., and Yamashita, T. (2005) *J. Neurochem.* **94,** 15–21
52. Venkatesh, K., Chivatakarn, O., Sheu, S. S., and Giger, R. J. (2007) *J. Cell Biol.* **177,** 393–399
53. Yamashita, K., Mizuochi, T., and Kobata, A. (1982) *Methods Enzymol.* **83,** 105–126
54. Svennerholm, L. (1994) *Prog. Brain Res.* **101,** xi–xiv

Gangliosides and Nogo Receptors Independently Mediate Myelin-associated Glycoprotein Inhibition of Neurite Outgrowth in Different Nerve Cells

Niraj R. Mehta, Pablo H. H. Lopez, Alka A. Vyas and Ronald L. Schnaar

J. Biol. Chem. 2007, 282:27875-27886.
doi: 10.1074/jbc.M704055200 originally published online July 19, 2007
